

Maher Ghazal, Uğur Atikol, and Fuat Egelioglu

Abstract

This work investigates the thermal performance of a solar humidification technique that is suitable to use in a Humidification Dehumidification Desalination system (HDD). Water heating and air humidification processes have been merged to take place in a direct contact water solar thermal collection unit. Experiments are conducted under the weather conditions of N. Cyprus. Air passes through brackish water in the humidifier and reaches saturation at the outlet. The difference between temperatures and relative humidity at the inlet and outlet of the humidifier were recorded for different airflow rates (8.2, 10.4, and 12.6 kg/h) between December 1 and 4, 2012. The experiment demonstrated that for an average solar radiation of 600 W/m^2 and a mass flow rate of 12.6 kg/h of air, the increase in average absolute humidity was 0.62 kg/h m^2 . As the airflow rate was stepped up, the rate of vapor transfer increased but the efficiency of the humidification process slightly dropped.

Keywords

Humidification • Solar thermal • Water heating • Water production • Desalination

Introduction

As the demand for fresh water is growing, scientists are proposing new methods for desalination. With the exponential growth in industry, techniques used in desalination have advanced too. Among all the desalination techniques known up to the present time, reverse osmosis and multistage flash systems are the most common ones in terms of large scale applications. On the other hand, medium and small scale desalination techniques are competing for the lead in terms of independency, reliability, productivity, and cost. The importance of the small scale plants manifests itself in the rural areas, countryside, and remote places.

This work focuses on one of the latest small scale desalination techniques known as humidification dehumidification desalination. HDD systems have had limited use in industry, due to their poor process efficiency caused by heat losses; however, their feasibility became more favorable with the use of solar energy.

Several works have been performed on solar HDD desalination systems, using different configurations. Prakash et al. [1] provided a comprehensive review on solar-driven humidification–dehumidification desalination. These systems varied between open and closed systems with heated air or heated water setups. The technique is versatile with the main idea being bringing dry air in contact with water to be humidified in an evaporator before passing it through a condenser in which air is dehumidified to give fresh water.

M. Ghazal (✉) • U. Atikol • F. Egelioglu

Department of Mechanical Engineering, Eastern Mediterranean University, via Mersin 10, Gazimagusa, North Cyprus, Turkey
e-mail: maher.ghazal@emu.edu.tr; ugur.atikol@emu.edu.tr; fuat.egelioglu@emu.edu.tr

This study investigates the moisture carrying capacity of air bubbles passing through water. In general, this setup compresses air into water through a pipe, which has several holes on its immersed end. The air exits the holes in the form of bubbles and then ascends vertically under the buoyancy effect. A similar experimental investigation has been carried out by El-Agouz [2] but on a system that uses electrical energy in order to heat sea water. The present study uses solar energy as the main energy source (i.e., energy used for water and air heating). The evaporation chamber and the solar water/air heater are combined into one unit, containing a glass and inclined towards the sun, to achieve water heating, air bubbles heating, and humidification at the same time.

In fact this technique is widely used by chemists to diffuse gasses in liquids in a system known as a column reactor. But these systems have a challenging problem called the coalescence of bubbles. Bubble coalescence takes place even at the generation point or while rising to the surface. Upon coalescence of bubbles the superficial gas–liquid contact area decreases and thus mass and heat transfer to the bubble decrease (i.e., humidification decreases).

In their study of the lower region of the bubble column, Perry and Green [3] found that bubble coalescence depends on the dispersion device. They claimed that in the bubble generator design, the typical separation between orifice centers should range from 2.5 to 4 times the orifice diameter. This result has been considered in the design of the bubble generator used in this study. The coalescence process has been studied in the central region of the bubble column by Camarasa et al. [4] and Pohorecki et al. [5] where bubble break-up and coalescence processes reach equilibrium. They have determined the bubble mean diameter was responsible for the superficial area available for transport phenomena between the gas phase and the liquid phase. It is evident from these studies that the smaller the bubble diameter, the greater the heat and mass transfer to it.

Martin et al. [6] studied the effect of coalescence of bubbles at sieve plate on mass transfer revealing that the results showed that although coalescence decreases mass transfer rate from bubbles, the deformable bubble generated can, in certain cases, balance the decrease in mass transfer rate due to the reduction in superficial area.

Chen et al. [7] investigated the coalescence of bubble pairs rising in a stagnant liquid numerically and compared the results with the experimental ones. The numerical results indicated that the rising velocity of the trailing bubble was larger than that of the leading bubble. They indicated that both of the leading bubble and the trailing bubble rose faster than the single bubble. This is in fact another factor that affects the rate of heat and mass transfer to the bubbles since faster rising bubbles decrease the interaction time and thus decreases the amount of heat and mass transferred.

The main objective of the present study is to investigate experimentally the result of merging the humidification and water heating processes of the HDD in an inclined solar collector bed. The effects of different parameters (i.e., temperatures and different air mass flow rates) on the moisture carrying capacity of air bubbles are also studied.

Experimental Setup

The experimental setup presented in this study comes with a new conceptual solar humidifier by which two stages of the HDD system are accomplished, namely heating and humidification. The major components that were used in the setup are the humidifier bed, the compressor, and the data retrieving devices, see Fig. 36.1. These components are briefly explained in the following sections.

The Humidifier Bed

The humidifier bed is made using Plexiglas for framing, galvanized metal sheet is used as an absorber, and glazing from glass sheets for the aperture. The whole bed then was insulated and enclosed in a wooden box, except the aperture side was glazed allowing sunlight to penetrate through onto the 2 mm absorber plate by which the water contained in the cavity was heated by solar energy. In order to withstand the pressure of water underneath the humidifier, the aperture is double glazed with 8 mm thick inner glass and 4 mm thick outer glass having width of 50 cm and length of 100 cm. A half inch diameter and 60 cm long copper pipe was inserted all the way through a hole, which was drilled from one side of the bed to the opposite side of the bed and was fixed internally. The pipe had 2 mm diameter holes drilled apart with 10 mm center-to-center distances along 500 mm of its length, which is immersed in the bed. The purpose of this pipe is to generate air bubbles into the water. The distance between the glazing and the absorber plate was 5 mm. Air exits the system through 1 in. diameter Plexiglas pipe attached to a hole in the upper part of the frame. The whole bed was mounted on a frame and was tilted due south to face the sun.

Fig. 36.1 The humidification system



Compressor and Controllers

An electrically driven two-piston compressor was used to supply air to the system. The compressor was equipped with a 200 L of storage tank, airflow controller, and pressure controllers to control the air in the tank as well as the inlet air to the system.

Data Acquisition and Measuring Devices

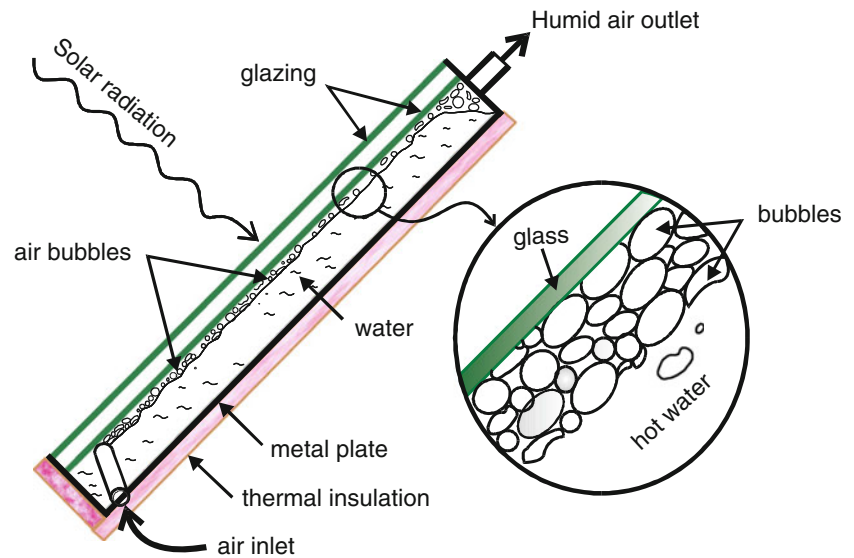
The data collected in this study was airflow rate, global solar radiation, water temperature, inlet and outlet air temperatures, and relative humidity. Solar intensity on the surface of the system was measured using a Pyranometer coupled with a digital multimeter. The Eppley radiometer Pyranometer has the accuracy of ± 0.5 for the range from 0 to $2,800 \text{ W/m}^2$. Water temperature was snapped using two thermocouples which were connected to Xplorer GLX data logger. Inlet and outlet relative humidity and temperatures of the air were acquired using an Omega Thermo Hygrometer RH411 with measurement range of 5–98 % relative humidity and 0–49 °C temperature. The measurement accuracy of the hygrometer is ± 0.8 °C for temperature and ± 3 % for relative humidity. The airflow rate was measured using a hot wire anemometer.

Experimental Procedure and Data Processing

Procedure

The main working principle is to bring unsaturated air (i.e., air bubbles) into contact with water to saturate the air in a process called humidification. In this setup air bubbles travel freely through still water in the cavity to ensure maximum contact surface area; thus, greater mass transfer rate can be achieved.

Fig. 36.2 Working principle of the humidifier



Water was filled in the cavity to about two-third in order to make room for the volume of the air bubbles. The south facing bed allowed the solar energy to penetrate through the glazing to the black painted absorber plate. The absorber in turn transferred the absorbed heat to the contained water and increased its temperature. Compressed air was directed through the copper pipe and bubbles were generated in the water. While ascending upwards, heat and mass transfer to the bubbles took place (Fig. 36.2).

Data of the solar intensity, water temperature, and air relative humidity and temperatures at the inlet and outlet of the evaporator were recorded hourly from 9:30 AM to 3:30 PM in mid-winter for three different airflow rates (8.2, 10.4, and 12.6 kg/h).

Data Processing

The absolute humidity calculation was made possible using the data snapped by the electronic Hygrometer. The inlet and outlet relative humidity and temperatures of air were inserted to a computer-aided thermodynamic table that gave all the thermodynamic properties of air including the most important of which, the absolute humidity. Then the difference between the inlet and outlet absolute humidity was calculated to determine the increase in water vapor content in air through the process. Humidification Process Efficiency η_h was determined according to the following consideration.

Humidification Process Efficiency is considered as the ratio of actual increment in humidity to the maximum possible increment in vapor content at the saturated temperature of air. Humidification Process Efficiency is given by:

$$\eta_h = 100 \frac{\omega_{out} - \omega_{in}}{\omega_{out@sat.air} - \omega_{in}} \quad (36.1)$$

Results and Discussion

Figure 36.3 shows the inlet and the outlet relative humidity of the air passing through the humidifier for different airflow rates (i.e., 8.2, 10.4, and 12.6 kg/h) on different days. Although the inlet relative humidity varied for each day, the outlet relative humidity was almost 100 % with slight decrease at flow rate of 12.6 kg/h.

Figure 36.4 shows the inlet and outlet temperatures of air as well as that of the water. It can be seen that there is a gap between the passing air temperature and water temperature for all of the flow rates. As the flow rate increases the difference between the inlet and outlet temperatures decreases. This behavior can be explained with two reasons: the first one is the chilling effect of air on water due to higher flow rate and thus higher heat transfer rate. The second reason is that the energy

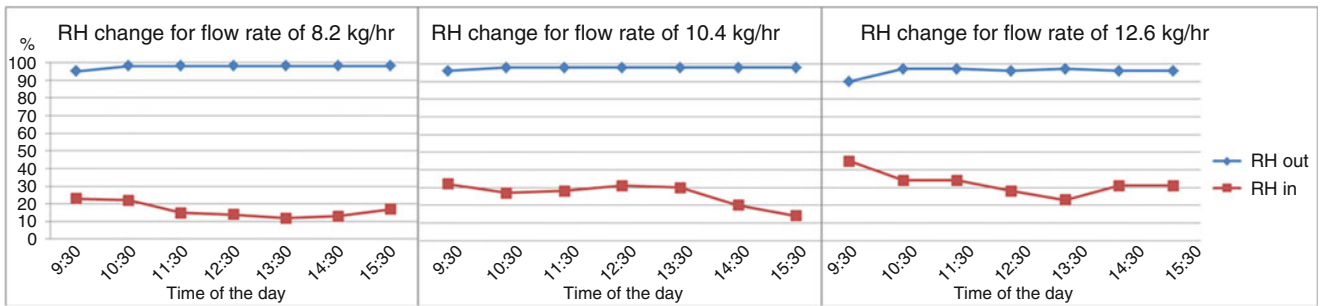


Fig. 36.3 The inlet and outlet relative humidity of air for different flow rates

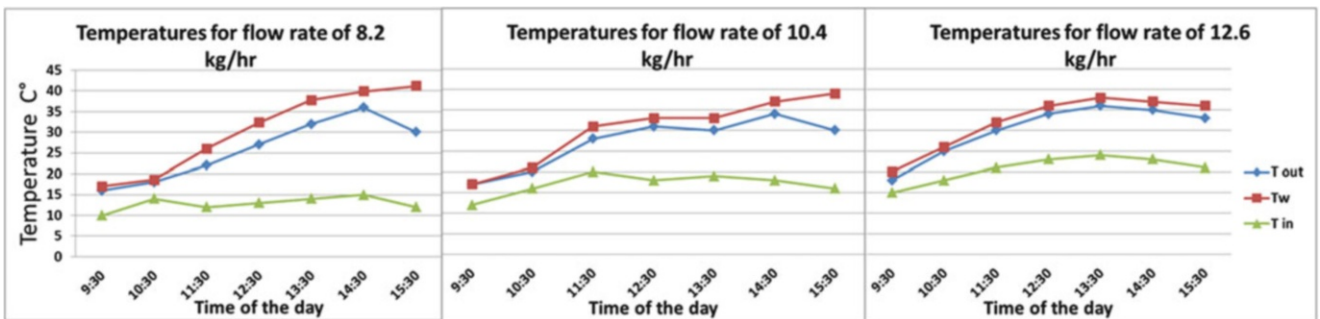


Fig. 36.4 Effect of airflow rate on the temperature differences between the air inlet and outlet

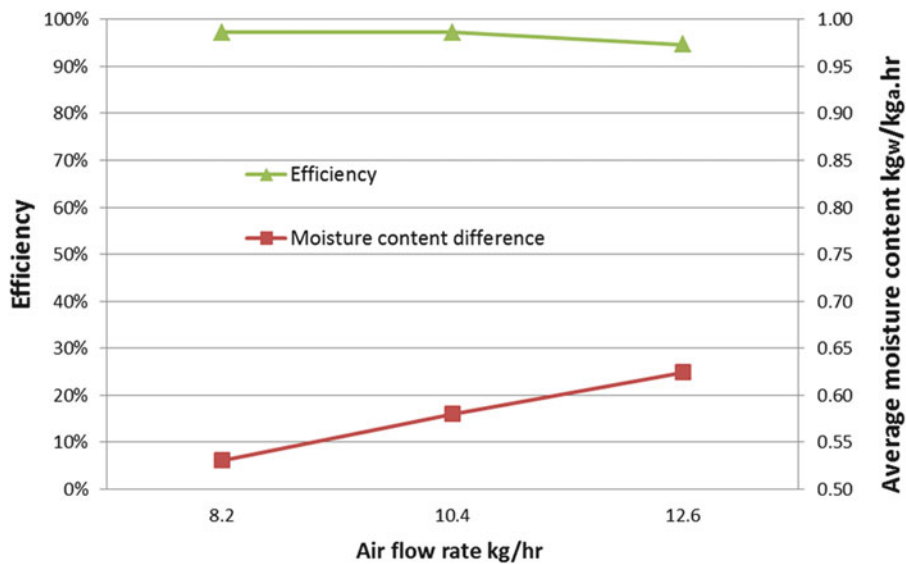


Fig. 36.5 Effect of higher flow rates on the productivity and humidification efficiency

of vaporization, which comes mainly from water, needed for phase change, increases as it is directly proportional to the amount of vaporized water which increases with the airflow rate.

Figure 36.5 illustrates the average moisture content differences between the inlet and outlet air for each flow rate (i.e., 8.2, 10.4, 12.6 kg/h) in addition to the average efficiency calculated using Eq. (36.1). It can be clearly seen that mass transferred is greater for greater flow rates whereas efficiency of the humidification process decreases slightly.

